OPTIMIZED MULTIPLICATIVE, ADDITIVE AND RESTRICTED ADDITIVE SCHWARZ PRECONDITIONING

A. ST-CYR *, M. J. GANDER†, AND S. J. THOMAS‡

Abstract. We demonstrate that a small modification of the multiplicative, additive and restricted additive Schwarz preconditioner at the algebraic level, motivated by optimized Schwarz methods defined at the continuous level, leads to a significant reduction in the iteration count of the iterative solver. Numerical experiments using finite difference and spectral element discretizations of the positive definite Helmholtz problem and an idealized climate simulation illustrate the effectiveness of the new approach.

Key words. Domain decomposition, restricted additive Schwarz method, optimized Schwarz methods, multiplicative Schwarz, spectral elements, high-order.

AMS subject classifications. 65F19, 65N22, 65N35

1. Introduction. The classical Schwarz method employs Dirichlet transmission conditions between subdomains. By introducing a more general Robin transmission condition, it is possible to optimize the convergence of the original algorithm, see [9] and the references therein. In this paper, general results are derived for using optimized transmission conditions at the algebraic level of restricted additive Schwarz (RAS), multiplicative Schwarz (MS) and additive Schwarz (AS) on an augmented system. These methods are then applied to the positive definite Helmholtz problem $(\eta - \Delta)u = f$, $\eta > 0$, discretized with finite differences and spectral finite elements, by a simple modification of already existing classical implementations of RAS, MS and AS, with and without overlap.

Optimized Schwarz methods were originally derived from Fourier analysis of the continuous elliptic partial differential equation, see [9] and references therein. Until now, it was not clear how to introduce optimized transmission conditions in the classical forms of the AS, MS and RAS preconditioners at the algebraic level. The present work closes this gap by showing that small modifications of the subdomain matrices in these preconditioners lead to optimized Schwarz methods. The modified preconditioners must satisfy specific compatibility conditions. For optimized RAS (ORAS), an overlap condition must be satisfied. In the case of optimized MS (OMS), there is no such condition on the overlap. Optimized AS (OAS) requires an augmented system, permitting the use of non-overlapping regions, where the common unknowns at subdomain boundaries are duplicated. Because these results are algebraic, they readily apply to any space discretization of continuous PDEs for which optimized Schwarz methods have been analyzed in the literature, see [9] for positive definite Helmholtz problems, [12, 10] for indefinite Helmholtz problems, and [14, 6] for advection diffusion problems. Greatly enhanced convergence factors have been shown for one level optimized Schwarz methods in these references at the continuous level, with much weaker dependence on the overlap than classical one level Schwarz methods. There are also first attempts to directly construct algebraically good transmission conditions, which are related to approximations of Schur complement matrices, see

*Corresponding author, NCAR 1850 Table Mesa Drive Boulder, CO 80305, USA, (amik@ucar.edu)

†Section de Mathématiques, Université de Genève, CP 64, CH-1211 Genève, (mgander@math.unige.ch)

‡NCAR 1850 Table Mesa Drive Boulder, CO 80305, USA, (thomas@ucar.edu)

[22, 17, 28, 11]. There are however no two level variants yet for optimized Schwarz methods.

Schwarz algorithms are reviewed in the following section, and the link between the discrete and continuous problems is established. The equivalence of the iterative forms of optimized Schwarz methods with ORAS and OMS is demonstrated for multiple domains, as well as with OAS applied to an augmented system. These results are then applied to the positive definite Helmholtz problem using finite difference and spectral element discretizations. The size of the overlap region is varied for finite differences, whereas non-overlapping subdomains are considered for spectral elements. We finally apply the new techniques to a spectral element climate model [27].

2. Classical Schwarz Methods. Schwarz methods for elliptic partial differential equations sub-divide the physical domain into subdomains and iterate the subdomain solutions in order to obtain the global solution. When the subdomain problems are discretized, Schwarz methods can be formulated at the discrete or algebraic level.

2.1. Schwarz Methods at the Algebraic Level. Discretization of the elliptic partial differential equation,

$$\mathcal{L}u = f \quad \text{in } \Omega, \quad \mathcal{B}u = g \quad \text{on } \partial\Omega, \tag{2.1}$$

where $\mathcal{L}$ is an elliptic differential operator, $\mathcal{B}$ is a boundary operator and Ω is a bounded domain, leads to a linear system of equations

$$A\boldsymbol{u} = \boldsymbol{f}. \tag{2.2}$$

A stationary iterative method for (2.2) is given by

$$\boldsymbol{u}^{n+1} = \boldsymbol{u}^n + M^{-1}(\boldsymbol{f} - A\boldsymbol{u}^n). \tag{2.3}$$

An initial guess $\boldsymbol{u}^0$ is required to start the iteration. Algebraic domain decomposition methods group the unknowns into subsets, $\boldsymbol{u}_j = R_j\boldsymbol{u}$, $j = 1, \ldots, J$, where R_j are rectangular restriction matrices such that each entry u_i of the vector $\boldsymbol{u}$ is contained in at least one $\boldsymbol{u}_j$. Coefficient matrices for subdomain problems are defined by $A_j = R_j A R_j^T$. The classical multiplicative Schwarz method (MS) is a stationary iteration (2.3) where the preconditioner M is

$$M_{MS}^{-1} = \left[I - \prod_{j=1}^{J} \left(I - R_j^T A_j^{-1} R_j A \right) \right] A^{-1}. \tag{2.4}$$

Multiplicative Schwarz is often written using fractional steps,

$$\boldsymbol{u}^{n+\frac{j}{J}} = \boldsymbol{u}^{n+\frac{j-1}{J}} + R_j^T A_j^{-1} R_j (\boldsymbol{f} - A\boldsymbol{u}^{n+\frac{j-1}{J}}), \quad j = 1, \ldots, J, \tag{2.5}$$

which shows that it is equivalent to a Gauss-Seidel iteration on the subdomains [25]. It thus corresponds to the original alternating method introduced by Schwarz at the continuous level [23]. A more parallel variant is the additive Schwarz (AS) preconditioner introduced in [5],

$$M_{AS}^{-1} = \sum_{j=1}^{J} R_j^T A_j^{-1} R_j. \tag{2.6}$$

In general, the additive Schwarz iteration (2.3), (2.6) does not converge, nor does it correspond to a classical iteration per subdomain, [7]. The Restricted Additive Schwarz method (RAS) [3] corrects this problem by introducing prolongation operators $\tilde{R}_j^T$, corresponding to a non-overlapping decomposition. Each entry u_i of the vector $\boldsymbol{u}$ occurs in $\tilde{R}_j\boldsymbol{u}$ for exactly one j. The RAS preconditioner is

$$M_{RAS}^{-1} = \sum_{j=1}^{J} \tilde{R}_j^T A_j^{-1} R_j. \tag{2.7}$$

Another way to alleviate the convergence problems of AS is to apply M_{AS} as a preconditioner in a Krylov iteration. In general, also MS and RAS will be accelerated by Krylov iteration.

The algebraic formulation of Schwarz methods has an important feature: a subdomain matrix A_j is not necessarily the restriction of A to a subdomain j. For example, if A represents a spectral element discretization of a differential operator, then A_j can be obtained from a finite element discretization on the Gaussian quadrature points. Furthermore subdomain matrices A_j can be chosen to accelerate convergence and this is the focus of the next section.

2.2. Schwarz Methods at the Continuous Level. Historically, domain decomposition methods were formulated at the continuous level. Consider a decomposition of the original domain Ω into two overlapping sub-domains Ω_1 and Ω_2, and denote the interfaces by $\Gamma_{ij} = \partial\Omega_i \cap \Omega_j$, $i \neq j$, and the outer boundaries by $\partial\Omega_j = \partial\Omega \cap \bar{\Omega}_j$.

The original alternating Schwarz method introduced in [23] for (2.1) is

$$\begin{array}{rclll} \mathcal{L}u_1^{n+1} & = & f & \text{in } \Omega_1, & \mathcal{L}u_2^{n+1} = f \quad \text{in } \Omega_2, \\ \mathcal{B}(u_1^{n+1}) & = & g & \text{on } \partial\Omega_1, & \mathcal{B}(u_2^{n+1}) = g \quad \text{on } \partial\Omega_2, \\ u_1^{n+1} & = & u_2^n & \text{on } \Gamma_{12}, & u_2^{n+1} = u_1^{n+1} \quad \text{on } \Gamma_{21}, \end{array} \tag{2.8}$$

corresponding to Gauss-Seidel traversal of the subdomains. The Jacobi variant of the algorithm introduced in [16] is

$$\begin{array}{rclll} \mathcal{L}u_1^{n+1} & = & f & \text{in } \Omega_1, & \mathcal{L}u_2^{n+1} = f \quad \text{in } \Omega_2, \\ \mathcal{B}(u_1^{n+1}) & = & g & \text{on } \partial\Omega_1, & \mathcal{B}(u_2^{n+1}) = g \quad \text{on } \partial\Omega_2, \\ u_1^{n+1} & = & u_2^n & \text{on } \Gamma_{12}, & u_2^{n+1} = u_1^n \quad \text{on } \Gamma_{21}. \end{array} \tag{2.9}$$

It was shown in [7] that the discrete form of (2.8), represented by

$$A_1\boldsymbol{u}_1^{n+1} = \boldsymbol{f}_1 + B_{12}\boldsymbol{u}_2^n, \quad A_2\boldsymbol{u}_2^{n+1} = \boldsymbol{f}_2 + B_{21}\boldsymbol{u}_1^{n+1}, \tag{2.10}$$

is equivalent to MS in (2.4), and that the discrete form of (2.9),

$$A_1\boldsymbol{u}_1^{n+1} = \boldsymbol{f}_1 + B_{12}\boldsymbol{u}_2^n, \quad A_2\boldsymbol{u}_2^{n+1} = \boldsymbol{f}_2 + B_{21}\boldsymbol{u}_1^n, \tag{2.11}$$

is equivalent to RAS in (2.7).

3. Optimized Schwarz Methods. Optimized Schwarz methods were developed at the continuous level using Fourier analysis and led to significantly faster convergence rates than classical Schwarz methods, [9]. An algebraic formulation of optimized Schwarz methods is lacking. Here it is shown how optimized Schwarz methods can be embedded within the framework of RAS, MS and AS.

3.1. Optimized Schwarz Methods at the Continuous Level. In optimized Schwarz methods, the Dirichlet transmission conditions on the interfaces Γ_{ij} in (2.8) and (2.9) are replaced by more effective conditions including derivatives. The latter permits the use of non-overlapping domains. The optimized algorithm for the classical case is

$$\begin{array}{rclll rclll} \mathcal{L}u_1^{n+1} & = & f & \text{in } \Omega_1, & & \mathcal{L}u_2^{n+1} & = & f & \text{in } \Omega_2, & \\ \mathcal{B}(u_1^{n+1}) & = & g & \text{on } \partial\Omega_1, & & \mathcal{B}(u_2^{n+1}) & = & g & \text{on } \partial\Omega_2, & (3.1) \\ \tilde{\mathcal{B}}_{12}u_1^{n+1} & = & \tilde{\mathcal{B}}_{12}u_2^{n} & \text{on } \Gamma_{12}, & & \tilde{\mathcal{B}}_{21}u_2^{n+1} & = & \tilde{\mathcal{B}}_{21}u_1^{n+1} & \text{on } \Gamma_{21}, & \end{array}$$

where the transmission operators $\mathcal{B}_{12}$ and $\mathcal{B}_{21}$ are chosen to obtain faster convergence. Similarly, the more parallel Jacobi version of the optimized Schwarz method is

$$\begin{array}{rclll rclll} \mathcal{L}u_1^{n+1} & = & f & \text{in } \Omega_1, & & \mathcal{L}u_2^{n+1} & = & f & \text{in } \Omega_2, & \\ \mathcal{B}(u_1^{n+1}) & = & g & \text{on } \partial\Omega_1, & & \mathcal{B}(u_2^{n+1}) & = & g & \text{on } \partial\Omega_2, & (3.2) \\ \tilde{\mathcal{B}}_{12}u_1^{n+1} & = & \tilde{\mathcal{B}}_{12}u_2^{n} & \text{on } \Gamma_{12}, & & \tilde{\mathcal{B}}_{21}u_2^{n+1} & = & \tilde{\mathcal{B}}_{21}u_1^{n} & \text{on } \Gamma_{21}. & \end{array}$$

The interface formulation was extensively tested in [9] for $\mathcal{L} = \eta - \Delta$, and optimized transmission conditions of Robin and second order type were developed leading to significantly faster convergence rates.

A discretization with optimized transmission conditions leads to discrete versions of the form (2.10) and (2.11). The subdomain matrices A_j are replaced by $\tilde{A}_j$ and the transmission operators B_{jk} are replaced by $\tilde{B}_{jk}$, corresponding to the optimized transmission conditions derived at the continuous level for various types of PDEs, see [9, 12, 10, 14, 6] and references therein.

3.2. Optimized Restricted Additive Schwarz Methods. The optimized restricted additive Schwarz method is based on the restricted additive Schwarz method (2.3) and (2.7), but uses different subdomain matrices, which come from the optimized Jacobi Schwarz method,

$$\tilde{A}_j \boldsymbol{u}_j^{n+1} = \boldsymbol{f}_j + \sum_{k=1}^{J} \tilde{B}_{jk} \boldsymbol{u}_k^n, \quad j = 1, .., J, \tag{3.3}$$

where $\tilde{B}_{jj} = 0$ to simplify the notation. We show that, for sufficient overlap, the subdomain matrices A_j in the RAS algorithm (2.3) and (2.7) can be replaced by the optimized subdomain matrices $\tilde{A}_j$ from (3.3) to obtain an optimized RAS method (ORAS),

$$\boldsymbol{u}^{n+1} = \boldsymbol{u}^n + (\sum_{j=1}^{J} \tilde{R}_j^T \tilde{A}_j^{-1} R_j)(\boldsymbol{f} - A\boldsymbol{u}^n), \tag{3.4}$$

which produces the same iterates as (3.3). An advantage of the ORAS implementation (3.4) over the optimized Schwarz method (3.3) is that the additional transmission operators $\tilde{B}_{jk}$ are not needed in ORAS, which greatly simplifies the transition from an existing RAS implementation to ORAS. For a simplified proof in the case of 2 subdomains and a link to the Schur complement system consult [28].

DEFINITION 3.1 (Consistency). *Let R_j, $j = 1, .., J$ be restriction operators covering the entire discrete domain, and let $\boldsymbol{f}_j = R_j \boldsymbol{f}$. The matrix splitting R_j, $\tilde{A}_j$, $\tilde{B}_{jk}$,*

$j = 1, ..., J$ and $k = 1, ..., J$ in (3.3) is consistent, if for all $\boldsymbol{f}$ and associated solution $\boldsymbol{u}$ of (2.2), $\boldsymbol{u}_j = R_j \boldsymbol{u}$ satisfy

$$\tilde{A}_j \boldsymbol{u}_j = \boldsymbol{f}_j + \sum_{k=1}^{J} \tilde{B}_{jk} \boldsymbol{u}_k. \tag{3.5}$$

LEMMA 3.2. *Let A in (2.2) have full rank. For a consistent matrix splitting R_j, $\tilde{A}_j$, $\tilde{B}_{jk}$, $j = 1, ..., J$ and $k = 1, ..., J$, we have the matrix identities*

$$\tilde{A}_j R_j - \sum_{k=1}^{J} \tilde{B}_{jk} R_k = R_j A, \quad j = 1, \ldots, J. \tag{3.6}$$

Proof. For an arbitrary $\boldsymbol{f}$, we apply R_j to equation (2.2), and obtain, using consistency (3.5),

$$R_j A \boldsymbol{u} = R_j \boldsymbol{f} = \boldsymbol{f}_j = \tilde{A}_j \boldsymbol{u}_j - \sum_{k=1}^{J} \tilde{B}_{jk} \boldsymbol{u}_k.$$

Now using $\boldsymbol{u}_j = R_j \boldsymbol{u}$ and $\boldsymbol{u}_k = R_k \boldsymbol{u}$ on the right-hand side yields

$$(\tilde{A}_j R_j - \sum_{k=1}^{J} \tilde{B}_{jk} R_k - R_j A) \boldsymbol{u} = 0.$$

Because $\boldsymbol{f}$ was arbitrary and A is invertible, the identity is true for all $\boldsymbol{u}$ and therefore the identity (3.6) is established. □

While the definition of consistency is simple, it has important consequences: if the classical submatrices are used, i.e. $\tilde{A}_j = A_j = R_j A R_j^T$, then the restriction operators R_j can be overlapping or non-overlapping, and with the associated B_{jk}, we obtain a consistent splitting R_j, A_j, B_{jk}, $j = 1, \ldots, J$, $k = 1, \ldots, J$. However, if alternative subdomain matrices $\tilde{A}_j$ are employed, then the restriction operators R_j must be such that the unknowns in $\boldsymbol{u}_j$ affected by the change in $\tilde{A}_j$ are also available in neighboring $\boldsymbol{u}_k$ to compensate via $\tilde{B}_{jk}$ in equation (3.5). Hence consistency implies for all non-classical splittings a condition on the overlap in the R_j. A further restriction on the overlap is necessary for the optimized RAS algorithm:

ASSUMPTION 1. *We assume that the restriction operators R_j and the prolongation operators $\tilde{R}_j^T$ from the optimized RAS method (3.4) and the transmission operators $\tilde{B}_{jk}$ from the optimized parallel Schwarz method (3.3) satisfy*

$$\tilde{B}_{jk} R_k \tilde{R}_m^T = 0, \quad m \neq k. \tag{3.7}$$

REMARK 1. *The conditions (3.7) in Assumption 1 relate the overlap to the operators $\tilde{B}_{jk}$. Classical Schwarz methods only employ interface values from neighboring subdomains, and thus these conditions are automatically satisfied. The optimized Schwarz operators $\tilde{B}_{jk}$ approximate derivatives, requiring values at the interface and neighboring points. The operators $\tilde{R}_j$ must not overwrite these values, hence the requirement of a small overlap in the ORAS formulation.*

LEMMA 3.3. *Let R_j, $j = 1, ..., J$, be restriction operators covering the entire discrete domain, and let $\tilde{R}_j$ be the corresponding RAS versions of these operators. If Assumption 1 holds, then $\tilde{B}_{jk} R_k \tilde{R}_k^T = \tilde{B}_{jk}$ for all $j = 1, \ldots, J$, $k = 1, \ldots, J$.*

Proof. We first note that by the non-overlapping definition of $\tilde{R}_j$, $j = 1, ..., J$, the identity matrix I can be written as

$$I = \sum_{j=1}^{J} \tilde{R}_j^T \tilde{R}_j = \sum_{j=1}^{J} \tilde{R}_j^T R_j. \tag{3.8}$$

Now multiplying for $m \neq k$ the identity $\tilde{B}_{jk} R_k \tilde{R}_m^T = 0$ on the right by R_m and substituting the term $\tilde{R}_m^T R_m$ using (3.8) leads to

$$\tilde{B}_{jk} R_k (I - \sum_{l \neq m} \tilde{R}_l^T R_l) = 0 \quad \Longrightarrow \quad \tilde{B}_{jk} R_k = \sum_{l \neq m} \tilde{B}_{jk} R_k \tilde{R}_l^T R_l,$$

which, using Assumption 1, gives $\tilde{B}_{jk} R_k = \tilde{B}_{jk} R_k \tilde{R}_k^T R_k$. Hence we obtain $(\tilde{B}_{jk} - \tilde{B}_{jk} R_k \tilde{R}_k^T) R_k = 0$ which completes the proof, because the restriction matrix R_k has full rank. ∎

We are now ready to prove the main result of this subsection:

THEOREM 3.4. *Let R_j, $\tilde{A}_j$, $\tilde{B}_{jk}$, $j = 1, .., J$ and $k = 1, ..., J$, be a consistent matrix splitting, and let $\tilde{R}_j$ be the corresponding RAS versions of R_j. If the initial iterates $\boldsymbol{u}_j^0$, $j = 1, ..., J$, of the optimized Jacobi Schwarz method (3.3) and the initial iterate $\boldsymbol{u}^0$ of the optimized RAS method (3.4) satisfy*

$$\boldsymbol{u}^0 = \sum_{j=1}^{J} \tilde{R}_j^T \boldsymbol{u}_j^0, \tag{3.9}$$

and if Assumption 1 holds, then the two methods (3.3) and (3.4) generate an identical sequence of iterates,

$$\boldsymbol{u}^n = \sum_{j=1}^{J} \tilde{R}_j^T \boldsymbol{u}_j^n. \tag{3.10}$$

REMARK 2. *While condition (3.9) is important to prove that the sequence of iterates of the two methods, and thus the two methods, are equivalent, one would in practice not need to compute an initial condition $\boldsymbol{u}^0$ from given initial conditions $\boldsymbol{u}_j^0$ or vice versa, even though this can be achived directly using the formula (3.9). Note that for given $\boldsymbol{u}^0$, the choice of the $\boldsymbol{u}_j^0$ is not unique: entires in $\boldsymbol{u}_j^0$ ereased by $\tilde{R}_j^T$ can be chosen arbitrarily.*

Proof. The proof is by induction. For $n = 0$, (3.10) follows by assumption (3.9) on the initial iterates. We now assume that $\boldsymbol{u}^n = \sum_{j=1}^{J} \tilde{R}_j^T \boldsymbol{u}_j^n$, and show that the identity (3.10) holds for $n + 1$. Applying Lemma 3.2 to the j-th term of the sum in (3.4), we obtain

$$\begin{aligned} \tilde{R}_j^T \tilde{A}_j^{-1} R_j (\boldsymbol{f} - A\boldsymbol{u}^n) &= \tilde{R}_j^T \tilde{A}_j^{-1} (\boldsymbol{f}_j - R_j A \boldsymbol{u}^n) \\ &= \tilde{R}_j^T \tilde{A}_j^{-1} (\boldsymbol{f}_j - (\tilde{A}_j R_j - \textstyle\sum_{k=1}^{J} \tilde{B}_{jk} R_k) \boldsymbol{u}^n) \\ &= \tilde{R}_j^T (\tilde{A}_j^{-1} \boldsymbol{f}_j - R_j \boldsymbol{u}^n + \tilde{A}_j^{-1} \textstyle\sum_{k=1}^{J} \tilde{B}_{jk} R_k \boldsymbol{u}^n). \end{aligned} \tag{3.11}$$

Substituting this expression into (3.4), and using the identity (3.8) leads to

$$\boldsymbol{u}^{n+1} = \sum_{j=1}^{J} \tilde{R}_j^T \tilde{A}_j^{-1} (\boldsymbol{f}_j + \sum_{k=1}^{J} \tilde{B}_{jk} R_k \boldsymbol{u}^n).$$

Now using the induction hypothesis to replace $\boldsymbol{u}^n$ by $\sum_{m=1}^{J} \tilde{R}_m^T \boldsymbol{u}_m^n$ on the right hand side, we obtain

$$\boldsymbol{u}^{n+1} = \sum_{j=1}^{J} \tilde{R}_j^T \tilde{A}_j^{-1} (\boldsymbol{f}_j + \sum_{k=1}^{J} \sum_{m=1}^{J} \tilde{B}_{jk} R_k \tilde{R}_m^T \boldsymbol{u}_m^n).$$

By Assumption 1, the inner sum over m vanishes except for $m = k$, and together with Lemma 3.3, the above relation becomes

$$\boldsymbol{u}^{n+1} = \sum_{j=1}^{J} \tilde{R}_j^T \tilde{A}_j^{-1} (\boldsymbol{f}_j + \sum_{k=1}^{J} \tilde{B}_{jk} R_k \tilde{R}_k^T \boldsymbol{u}_k^n) = \sum_{j=1}^{J} \tilde{R}_j^T \tilde{A}_j^{-1} (\boldsymbol{f}_j + \sum_{k=1}^{J} \tilde{B}_{jk} \boldsymbol{u}_k^n).$$

Finally, using (3.3), we find

$$\boldsymbol{u}^{n+1} = \sum_{j=1}^{J} \tilde{R}_j^T \boldsymbol{u}_j^{n+1}$$

which concludes the proof by induction. □

3.3. Optimized Multiplicative Schwarz Methods. The optimized multiplicative Schwarz method (OMS) is an alternative to ORAS. In contrast to ORAS with an additional condition on the overlap, the consistency of the splitting suffices here. However OMS needs a coloring of subdomains to remain a parallel method. To implement a parallel optimized Schwarz method without conditions on the overlap, an augmented formulation is required, as shown in Subsection 3.4.

The optimized multiplicative Schwarz method is based on the multiplicative Schwarz method (2.5), but uses different subdomain matrices, which come from the discretized optimized alternating Schwarz method

$$\tilde{A}_j \boldsymbol{u}_j^{n+1} = \boldsymbol{f}_j + \sum_{k=1}^{j-1} \tilde{B}_{jk} \boldsymbol{u}_k^{n+1} + \sum_{k=j+1}^{J} \tilde{B}_{jk} \boldsymbol{u}_k^n, \quad j = 1, \ldots, J. \tag{3.12}$$

This method differs from (3.3), because subdomain solves are performed in a Gauss-Seidel fashion. The multiplicative Schwarz method (2.5) always uses the most recently updated values in the iteration by definition. To guarantee the same property for the alternating Schwarz method (3.12), we need an assumption which states this in mathematical terms:

ASSUMPTION 2. *We assume that the restriction operators R_j and the transmission operators $\tilde{B}_{jk}$ in the alternating Schwarz method (3.12) satisfy*

$$\tilde{B}_{jk} R_k R_m^T = 0$$

for all $j = 1, \ldots, J$ and

$$k \neq \begin{cases} j-1 & \text{if } j > 1, \\ J & \text{otherwise,} \end{cases} \qquad m \in \begin{cases} \{1, \ldots, j-1, k+1, \ldots, J\} & \text{if } k > j, \\ \{k+1, \ldots, j-1\} & \text{otherwise.} \end{cases}$$

REMARK 3. *Assumption 2 looks deceivingly similar to the overlap Assumption 1 in the ORAS method, but it is not a constraint on the overlap. It simply states that the most recently updated values must be used by the transmission operators $\tilde{B}_{jk}$ in (3.12), i.e. we need $\tilde{B}_{jk}R_kR_m^T = 0$, if values from subdomain m have been updated more recently than from subdomain k, which with the ordering implied by (3.12), leads to the conditions in Assumption 2.*

We now show that replacing the subdomain matrices A_j, $j = 1, \ldots, J$ in the multiplicative Schwarz method (2.5) by their optimized variants $\tilde{A}_j$ from (3.12), the new OMS method

$$\boldsymbol{u}^{n+\frac{j}{J}} = \boldsymbol{u}^{n+\frac{j-1}{J}} + R_j^T \tilde{A}_j^{-1} R_j (\boldsymbol{f} - A\boldsymbol{u}^{n+\frac{j-1}{J}}), \quad j = 1, \ldots, J \tag{3.13}$$

produces the same iterates as (3.12), again without the explicit use of the transmission operators $\tilde{B}_{jk}$. Three lemmas are needed to prove this result.

LEMMA 3.5. *For $j = 1, \ldots, J$, the matrix identity $R_j(I - R_j^T R_j) = 0$ holds.*

Proof. The result follows by multiplying through by R_j,

$$R_j(I - R_j^T R_j) = (R_j - R_j R_j^T R_j) = (I - R_j R_j^T)R_j = 0,$$

because $R_j R_j^T = I$. ∎

LEMMA 3.6. *For overlapping or non-overlapping restriction operators R_j, $j = 1, \ldots, J$ covering the entire domain, we have*

$$\prod_{j=1}^{J} (I - R_j^T R_j) = 0.$$

Proof. For $A \in \mathbb{R}^{m \times m}$, the rectangular Boolean matrices R_j are of dimensions $n_j \times m$ and have rank n_j. Let S_j be the index set formed by the integers representing columns of R_j containing a 1. Since the restriction operators R_j are covering the entire domain, we have $\cup_{j=1}^{J} S_j = \{1, 2, 3, ..., m\} \equiv M$. If we denote for the index set S by I_S the matrix with ones on the diagonal indicated by the indices in S, and zeros everywhere else, we have $I_{S_j^c} = I - R_j^T R_j$, where S_j^c denotes the complement of S_j in M. We now obtain

$$\prod_{j=1}^{J} (I - R_j^T R_j) = \prod_{j=1}^{J} I_{S_j^c} = I_{\cap_{j=1}^{J} S_j^c} = 0,$$

since $\cap_{j=1}^{J} S_j^c = (\cup_{j=1}^{J} S_j)^c = M^c = \emptyset$ by De Morgan's law. ∎

LEMMA 3.7. *For any given set of subdomain vectors $\boldsymbol{u}_l$, $l = 1, \ldots, J$ and under Assumption 2 we have:*

$$\tilde{B}_{jk} R_k \sum_{l=1}^{j-1} \prod_{i=l+1}^{j-1} (I - R_i^T R_i) R_l^T \boldsymbol{u}_l = \begin{cases} \tilde{B}_{jk}\boldsymbol{u}_k & \text{if } k < j, \\ 0 & \text{otherwise,} \end{cases} \tag{3.14}$$

and

$$\tilde{B}_{jk} R_k \prod_{i=1}^{j-1} (I - R_i^T R_i) \left(\sum_{p=1}^{J} \prod_{q=p+1}^{J} (I - R_q^T R_q) R_p^T \boldsymbol{u}_p \right) = \begin{cases} \tilde{B}_{jk}\boldsymbol{u}_k & \text{if } k > j, \\ 0 & \text{otherwise.} \end{cases} \tag{3.15}$$

Proof. We first start by showing (3.14): if $k < j$, we split the left hand side in (3.14) into three parts,

$$\begin{aligned}\tilde{B}_{jk}R_k\sum_{l=1}^{j-1}\prod_{i=l+1}^{j-1}(I-R_i^TR_i)R_l^T\boldsymbol{u}_l &= \sum_{l=1}^{k-1}\tilde{B}_{jk}R_k\prod_{i=l+1}^{j-1}(I-R_i^TR_i)R_l^T\boldsymbol{u}_l \\ +\tilde{B}_{jk}R_k\prod_{i=k+1}^{j-1}(I-R_i^TR_i)R_k^T\boldsymbol{u}_k &+ \sum_{l=k+1}^{j-1}\tilde{B}_{jk}R_k\prod_{i=l+1}^{j-1}(I-R_i^TR_i)R_l^T\boldsymbol{u}_l.\end{aligned} \tag{3.16}$$

The first sum on the right vanishes, because $k < j$ and the product includes the term $i = k$, and because the product terms commute, each term in the sum contains $R_k(I - R_k^TR_k)$ which is identically zero by Lemma 3.5. In the second term, on the right, in (3.16), two cases need to be distinguished: if $k = j - 1$, then the product is empty, and because $R_kR_k^T = I$, the term equals $\tilde{B}_{jk}\boldsymbol{u}_k$. On the other hand, if $k < j - 1$, we obtain

$$\tilde{B}_{jk}R_k\prod_{i=k+1}^{j-1}(I-R_i^TR_i)R_k^T\boldsymbol{u}_k = \tilde{B}_{jk}R_kR_k^T\boldsymbol{u}_k = \tilde{B}_{jk}\boldsymbol{u}_k,$$

where the assumption that $\tilde{B}_{jk}R_kR_i^T = 0$ for $k < j - 1$ and $i \in \{k + 1, \ldots, j - 1\}$ was used leading to $R_kR_k^T = I$. Hence, the second term always equals $\tilde{B}_{jk}\boldsymbol{u}_k$. Now for the last term in (3.16), two cases are again possible: if $k = j - 1$, then the sum is empty and thus the term is zero. If $k < j - 1$, then

$$\sum_{l=k+1}^{j-1}\tilde{B}_{jk}R_k\prod_{i=l+1}^{j-1}(I-R_i^TR_i)R_l^T\boldsymbol{u}_l = \sum_{l=k+1}^{j-1}\tilde{B}_{jk}R_kR_l^T\boldsymbol{u}_l = 0,$$

because again by assumption $\tilde{B}_{jk}R_kR_i^T = 0$ for $k < j - 1$ and $i \in \{k + 1, \ldots, j - 1\}$, and also $\tilde{B}_{jk}R_kR_l^T = 0$ for $k < j - 1$ and $l \in \{k + 1, \ldots, j - 1\}$, which concludes the proof for the first result (3.14) if $k < j$. Now if $k = j$, then the left hand side of (3.14) is zero because by definition $\tilde{B}_{jj} = 0$. Finally, if $k > j$, zero is obtained for $j = 1$, because the sum is empty, and for $j > 1$

$$\sum_{l=1}^{j-1}\tilde{B}_{jk}R_k\prod_{i=l+1}^{j-1}(I-R_i^TR_i)R_l^T\boldsymbol{u}_l = \sum_{l=1}^{j-1}\tilde{B}_{jk}R_kR_l^T\boldsymbol{u}_l = 0,$$

where the assumption $\tilde{B}_{jk}R_kR_i^T = 0$ for $k > j$ and $i \in \{2, \ldots, j-1\}$ and $\tilde{B}_{jk}R_kR_l^T = 0$ for $k > j$ and $l \in \{1, \ldots, j-1\}$ was again employed. This concludes the proof of (3.14).

To show the second identity (3.15), first note that for $k \leq j$,

$$\tilde{B}_{jk}R_k\prod_{i=1}^{j-1}(I-R_i^TR_i) = 0,$$

because for $k = j$, $\tilde{B}_{jk} = 0$, and for $k < j$ the product includes the term $R_k(I-R_k^TR_k)$ which is identically zero by Lemma 3.5. Now if $k > j$, then

$$\tilde{B}_{jk}R_k\prod_{i=1}^{j-1}(I-R_i^TR_i) = \tilde{B}_{jk}R_k,$$

because for $j = 1$ the product is empty, and for $j > 1$, we have by assumption $\tilde{B}_{jk} R_k R_i^T = 0$ for $k > j$ and $i \in \{1, \ldots, j-1\}$. The remaining sum is separated into three terms,

$$\tilde{B}_{jk} R_k \sum_{p=1}^{J} \prod_{q=p+1}^{J} (I - R_q^T R_q) R_p^T \boldsymbol{u}_p = \sum_{p=1}^{k-1} \tilde{B}_{jk} R_k \prod_{q=p+1}^{J} (I - R_q^T R_q) R_p^T \boldsymbol{u}_p$$
$$+ \tilde{B}_{jk} R_k \prod_{q=k+1}^{J} (I - R_q^T R_q) R_k^T \boldsymbol{u}_k + \sum_{p=k+1}^{J} \tilde{B}_{jk} R_k \prod_{q=p+1}^{J} (I - R_q^T R_q) R_p^T \boldsymbol{u}_p. \tag{3.17}$$

The first term on the right vanishes, because the product always contains the term $i = k$, and because the product terms commute, each term in the sum contains $R_k(I - R_k^T R_k)$ which is identically zero by Lemma 3.5. The second term on the right in (3.17) simplifies to

$$\tilde{B}_{jk} R_k \prod_{q=k+1}^{J} (I - R_q^T R_q) R_k^T \boldsymbol{u}_k = \tilde{B}_{jk} R_k R_k^T \boldsymbol{u}_k = \tilde{B}_{jk} \boldsymbol{u}_k,$$

because by assumption for $k > j$ and $k \neq J$ we have $\tilde{B}_{jk} R_k R_q^T = 0$ for $q \in \{k+1, \ldots, J\}$, and for $k = J$ the product is empty. Finally the last term in (3.17) becomes

$$\sum_{p=k+1}^{J} \tilde{B}_{jk} R_k \prod_{q=p+1}^{J} (I - R_q^T R_q) R_p^T \boldsymbol{u}_p = \sum_{p=k+1}^{J} \tilde{B}_{jk} R_k R_p^T \boldsymbol{u}_p = 0,$$

because for $k = J$ the sum is empty, and for $j < k < J$, by assumption, $\tilde{B}_{jk} R_k R_q^T = 0$ for $q \in \{k+2, \ldots, J\}$ and also $\tilde{B}_{jk} R_k R_p^T = 0$ for $p \in \{k+1, \ldots, J\}$, which concludes the proof. □

THEOREM 3.8. *Let R_j, $\tilde{A}_j$, $\tilde{B}_{jk}$, $j = 1, \ldots, J$, $k = 1, \ldots, J$ be a consistent matrix splitting. If the initial iterates $\boldsymbol{u}_j^0$, $j = 1, \ldots, J$ of the optimized Schwarz method (3.12) and the initial iterate $\boldsymbol{u}^0$ of the optimized multiplicative Schwarz method (3.13) satisfy*

$$\boldsymbol{u}^0 = \sum_{j=1}^{J} \prod_{i=j+1}^{J} (I - R_i^T R_i) R_j^T \boldsymbol{u}_j^0, \tag{3.18}$$

and Assumption 2 holds, then (3.12) and (3.13) generate an equivalent sequence of iterates,

$$\boldsymbol{u}^n = \sum_{j=1}^{J} \prod_{i=j+1}^{J} (I - R_i^T R_i) R_j^T \boldsymbol{u}_j^n, \tag{3.19}$$

Proof. The proof has two steps, both shown by induction. We first assume that for a fixed n, relation (3.19) holds, and show by induction that this implies the relation

$$\boldsymbol{u}^{n+\frac{j}{J}} = \prod_{i=1}^{j} (I - R_i^T R_i) \boldsymbol{u}^n + \sum_{l=1}^{j} \prod_{i=l+1}^{j} (I - R_i^T R_i) R_l^T \boldsymbol{u}_l^{n+1} \tag{3.20}$$

for $j = 0, 1, \ldots, J$. This relation trivially holds for $j = 0$. Assuming that it holds for $j-1$, we find from (3.13) using the matrix identity (3.6)

$$\begin{aligned}
\boldsymbol{u}^{n+\frac{j}{J}} &= \boldsymbol{u}^{n+\frac{j-1}{J}} + R_j^T \tilde{A}_j^{-1} R_j (\boldsymbol{f} - A\boldsymbol{u}^{n+\frac{j-1}{J}}) \\
&= \boldsymbol{u}^{n+\frac{j-1}{J}} + R_j^T \tilde{A}_j^{-1} (\boldsymbol{f}_j - \tilde{A}_j R_j \boldsymbol{u}^{n+\frac{j-1}{J}} + \sum_{k=1}^{J} \tilde{B}_{jk} R_k \boldsymbol{u}^{n+\frac{j-1}{J}}) \\
&= (I - R_j^T R_j) \boldsymbol{u}^{n+\frac{j-1}{J}} + R_j^T \tilde{A}_j^{-1} (\boldsymbol{f}_j + \sum_{k=1}^{J} \tilde{B}_{jk} R_k \boldsymbol{u}^{n+\frac{j-1}{J}}).
\end{aligned}$$

Now replacing relation (3.20) at $j-1$ in the last sum, together with Lemma 3.7, leads to

$$\begin{aligned}
\sum_{k=1}^{J} \tilde{B}_{jk} R_k \boldsymbol{u}^{n+\frac{j-1}{J}} &= \sum_{k=1}^{J} \tilde{B}_{jk} R_k (\prod_{i=1}^{j-1} (I - R_i^T R_i) \boldsymbol{u}^n + \sum_{l=1}^{j-1} \prod_{i=l+1}^{j-1} (I - R_i^T R_i) R_l^T \boldsymbol{u}_l^{n+1})) \\
&= \sum_{k=1}^{j-1} \tilde{B}_{jk} \boldsymbol{u}_k^{n+1} + \sum_{k=j+1}^{J} \tilde{B}_{jk} \boldsymbol{u}_k^n.
\end{aligned}$$

Substituting this result back into the expression for $\boldsymbol{u}^{n+\frac{j}{J}}$, we find, using (3.12) and relation (3.20) at $j-1$ again

$$\begin{aligned}
\boldsymbol{u}^{n+\frac{j}{J}} &= (I - R_j^T R_j) \boldsymbol{u}^{n+\frac{j-1}{J}} + R_j^T \tilde{A}_j^{-1} (\boldsymbol{f}_j + \sum_{m=1}^{j-1} \tilde{B}_{jk} \boldsymbol{u}_k^{n+1} + \sum_{m=j+1}^{J} \tilde{B}_{jk} \boldsymbol{u}_k^n) \\
&= \prod_{i=1}^{j} (I - R_i^T R_i) \boldsymbol{u}^n + \sum_{l=1}^{j-1} \prod_{i=l+1}^{j} (I - R_i^T R_i) R_l^T \boldsymbol{u}_l^{n+1} + R_j^T \boldsymbol{u}_j^{n+1} \\
&= \prod_{i=1}^{j} (I - R_i^T R_i) \boldsymbol{u}^n + \sum_{l=1}^{j} \prod_{i=l+1}^{j} (I - R_i^T R_i) R_l^T \boldsymbol{u}_l^{n+1},
\end{aligned}$$

which concludes the first proof by induction. The main result (3.19) can now be proved by induction on n. By the assumption on the initial iterate, (3.19) holds for $n = 0$. Thus assuming it holds for n, we obtain from the first part for this n, that relation (3.20) holds for $j = 0, 1, \ldots, J$. In particular, for $j = J$, we have

$$\boldsymbol{u}^{n+1} = \prod_{i=1}^{J} (I - R_i^T R_i) \boldsymbol{u}^n + \sum_{l=1}^{J} \prod_{i=l+1}^{J} (I - R_i^T R_i) R_l^T \boldsymbol{u}_l^{n+1},$$

and by Lemma 3.6 the first product vanishes, which completes the proof. □

3.4. Optimized Additive Schwarz Methods for the Augmented System. To obtain parallel discrete optimized Schwarz methods, which in contrast to ORAS can be used in a non-overlapping fashion, we need to introduce an augmented system, where unknowns in the overlap and at the interfaces are stored for each subdomain. Tang [29] called this an *enhanced* system, whereas the term *augmented* system was employed in [33].

At convergence, observe that the discretized optimized Schwarz method (3.3) leads naturally to the augmented system

$$\begin{bmatrix} \tilde{A}_1 & -\tilde{B}_{12} & \cdots & -\tilde{B}_{1,J-1} & -\tilde{B}_{1,J} \\ -\tilde{B}_{21} & \tilde{A}_2 & -\tilde{B}_{23} & \cdots & -\tilde{B}_{2,J} \\ \vdots & & \ddots & & \vdots \\ -\tilde{B}_{J-1,1} & \cdots & -\tilde{B}_{J-1,J-2} & \tilde{A}_{J-1} & -\tilde{B}_{J-1,J} \\ -\tilde{B}_{J,1} & -\tilde{B}_{J,2} & \cdots & -\tilde{B}_{J,J-1} & \tilde{A}_J \end{bmatrix} \begin{bmatrix} \boldsymbol{u}_1 \\ \boldsymbol{u}_2 \\ \vdots \\ \boldsymbol{u}_{J-1} \\ \boldsymbol{u}_J \end{bmatrix} = \begin{bmatrix} \boldsymbol{f}_1 \\ \boldsymbol{f}_2 \\ \vdots \\ \boldsymbol{f}_{J-1} \\ \boldsymbol{f}_J \end{bmatrix},$$

or in matrix notation, specifying augmented quantities by a hat,

$$\hat{A}\hat{\boldsymbol{u}} = \hat{\boldsymbol{f}}. \tag{3.21}$$

Applying a standard additive Schwarz method with non-overlapping restriction operators $\hat{R}_j$, to the augmented system (3.21), $\boldsymbol{u}_j = \hat{R}_j\hat{\boldsymbol{u}}$, we obtain the iterative method

$$\hat{\boldsymbol{u}}^{n+1} = \hat{\boldsymbol{u}}^n + \sum_{j=1}^{J} \hat{R}_j^T \tilde{A}_j^{-1} \hat{R}_j(\hat{\boldsymbol{f}} - \hat{A}\hat{\boldsymbol{u}}^n). \tag{3.22}$$

Note that the non-overlapping restriction operators $\hat{R}_j$ are related to the restriction operators for the consistent splitting R_j, $\tilde{A}_j$, $\tilde{B}_j$, $j = 1, ..., J$: their range is the same, only their domain is enlarged to account for the augmented matrix $\hat{A}$.

THEOREM 3.9. *Let R_j, $\tilde{A}_j$, $\tilde{B}_{jk}$, $j = 1, ..., J$, $k = 1, ..., J$ be a consistent matrix splitting. If the initial iterates $\boldsymbol{u}_j^0$, $j = 1, ..., J$ of the optimized Jacobi Schwarz method (3.3) and the initial iterate $\hat{\boldsymbol{u}}^0$ of the additive Schwarz method applied to the augmented system (3.22) satisfy*

$$\hat{\boldsymbol{u}}^0 = \left[(\boldsymbol{u}_1^0)^T,\ (\boldsymbol{u}_2^0)^T,\ \ldots\ (\boldsymbol{u}_J^0)^T\right]^T, \tag{3.23}$$

then (3.3) and (3.22) generate the same sequence of iterates, i.e.

$$\hat{\boldsymbol{u}}^n = \left[(\boldsymbol{u}_1^n)^T,\ (\boldsymbol{u}_2^n)^T,\ \ldots\ (\boldsymbol{u}_J^n)^T\right]^T. \tag{3.24}$$

Proof. The proof is again by induction. By assumption, (3.24) holds for $n = 0$. Assuming it holds for n, we obtain from (3.22), using the fact that the restriction operators $\hat{R}_j$, $j = 1, \ldots, J$ are non-overlapping, Lemma 3.2 and (3.3)

$$\begin{aligned} \hat{\boldsymbol{u}}^{n+1} &= \hat{\boldsymbol{u}}^n + \sum_{j=1}^{J} \hat{R}_j^T \tilde{A}_j^{-1} \hat{R}_j(\hat{\boldsymbol{f}} - \hat{A}\hat{\boldsymbol{u}}^n) = \hat{\boldsymbol{u}}^n + \sum_{j=1}^{J} \hat{R}_j^T \tilde{A}_j^{-1}(\boldsymbol{f}_j - \hat{R}_j\hat{A}\hat{\boldsymbol{u}}^n) \\ &= \hat{\boldsymbol{u}}^n + \sum_{j=1}^{J} \hat{R}_j^T \tilde{A}_j^{-1}(\boldsymbol{f}_j - \tilde{A}_j\boldsymbol{u}_j^n + \sum_{l=1}^{J} \tilde{B}_{jl}\boldsymbol{u}_l^n) = \sum_{j=1}^{J} \hat{R}_j^T \tilde{A}_j^{-1}(\boldsymbol{f}_j + \sum_{l=1}^{J} \tilde{B}_{jl}\boldsymbol{u}_l^n) \\ &= \sum_{j=1}^{J} \hat{R}_j^T \boldsymbol{u}_j^{n+1} = \left[(\boldsymbol{u}_1^{n+1})^T,\ (\boldsymbol{u}_2^{n+1})^T,\ \ldots\ (\boldsymbol{u}_J^{n+1})^T\right]^T = \hat{\boldsymbol{u}}^{n+1}, \end{aligned} \tag{3.25}$$

which concludes the proof. ∎

An advantage of this formulation is that non-overlapping parallel preconditioners can be used, such as the optimized Jacobi Schwarz method (3.3) and optimized alternating Schwarz method (3.12). A disadvantage is that the operators $\tilde{B}_{jk}$ must be constructed explicitly, because they are needed in the application of $\tilde{A}_j^{-1}$ in (3.22).

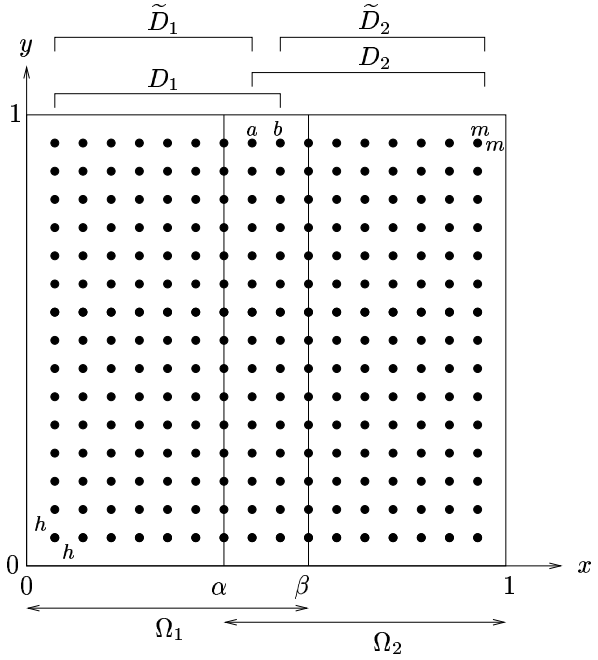

FIG. 4.1. *Finite difference discretization points and a two subdomain decomposition.*

4. Application to the positive definite Helmholtz Problem. We now apply the results of the previous sections to finite difference and spectral element discretizations of the positive definite Helmholtz problem on the domain Ω,

$$\mathcal{L}u = (\eta - \Delta)u = f, \quad \text{in } \Omega, \tag{4.1}$$

where Ω is an open set in two dimensions, and we impose homogeneous Dirichlet conditions to simplify the exposition.

4.1. Finite Differences. Discretizing (4.1) using a standard five point discretization on an equidistant grid on the domain $\Omega = (0,1) \times (0,1)$, as shown in Figure 4.1, and using a lexicographic ordering enumerating the unknowns from bottom to top and left to right leads to the matrix problem

$$A\boldsymbol{u} = \boldsymbol{f}, \quad A = \frac{1}{h^2}\begin{bmatrix} T_\eta & -I & \\ -I & T_\eta & \ddots \\ & \ddots & \ddots \end{bmatrix}, \quad T_\eta = \begin{bmatrix} \eta h^2 + 4 & -1 & \\ -1 & \eta h^2 + 4 & \ddots \\ & \ddots & \ddots \end{bmatrix},$$

where $A \in \mathbb{R}^{m^2 \times m^2}$, $T_\eta \in \mathbb{R}^{m \times m}$, $I \in \mathbb{R}^{m \times m}$ denotes the identity matrix, and $h = \frac{1}{m+1}$. Decomposing the domain Ω into the two subdomains $\Omega_1 = (0,\beta) \times (0,1)$ and $\Omega_2 = (\alpha,1) \times (0,1)$, as indicated in Figure 4.1, we obtain the rectangular restriction matrices $R_1 \in \mathbb{R}^{mb \times m^2}$ and $R_2 \in \mathbb{R}^{m(m-a+1) \times m^2}$ of the form $R_1 = [I\ 0]$ and $R_2 = [0\ I]$, where the ones in the identity matrices I of appropriate size correspond to the grid points indicated in Figure 4.1 by D_1 and D_2 respectively. The new restriction matrices $\tilde{R}_j$ are of the same size and form as R_j, $j = 1,2$, but have ones only on the diagonals for the grid points indicated by the nonoverlapping $\tilde{D}_j$

	p	q
TO0	$\sqrt{\eta}$	0
TO2	$\sqrt{\eta}$	$\frac{1}{2\sqrt{\eta}}$
OO0, no overlap	$\sqrt{\pi}(k_{\min}^2+\eta)^{1/4}h^{-1/2}$	0
OO0, overlap Ch	$2^{-1/3}(k_{\min}^2+\eta)^{1/3}(Ch)^{-1/3}$	0
OO2, no overlap	$2^{-1/2}\pi^{1/4}(k_{\min}^2+\eta)^{3/8}h^{-1/4}$	$2^{-1/2}\pi^{-3/4}(k_{\min}^2+\eta)^{-1/8}h^{3/4}$
OO2, overlap Ch	$2^{-3/5}(k_{\min}^2+\eta)^{2/5}(Ch)^{-1/5}$	$2^{-1/5}(k_{\min}^2+\eta)^{-1/5}(Ch)^{3/5}$

TABLE 4.1

Hierarchy of choices for the parameters p and q in the new interface blocks $\tilde{T}$ in (4.2). Here, TOj stands for Taylor of order j, and OOj stands for optimized of order j.

in Figure 4.1. The classical subdomain matrices associated with this decomposition are by definition $A_j = R_j A R_j^T$, $j = 1,2$, which implies that $A_1 \in \mathbb{R}^{mb\times mb}$ and $A_2 \in \mathbb{R}^{m(m-a+1)\times m(m-a+1)}$.

To obtain optimized RAS, MS and AS methods, it suffices according to the results in Section 3 to simply replace the classical subdomain matrices A_j by optimized subdomain matrices $\tilde{A}_j$ from optimized Schwarz methods. Since one changes only the transmission conditions to obtain optimized Schwarz methods, it suffices to replace the last diagonal block T_η in A_1, which is an interface block to the second subdomain, and the first diagonal block T_η in A_2, which is an interface block to the first subdomain, by the blocks corresponding to optimized transmission conditions, to obtain the optimized subdomain matrices $\tilde{A}_j$. We choose here interface blocks based on the continuous analysis of the underlying PDE and transmission conditions [9], which suggests replacing the two interface blocks T_η by the matrix

$$\tilde{T} = \frac{1}{2}T_\eta + phI + \frac{q}{h}(T_0 - 2I), \quad T_0 = T_\eta|_{\eta=0}, \tag{4.2}$$

which corresponds to a general optimized transmission condition of order 2 with two parameters p and q, see [9]. The optimal choice for the parameters p and q in the new block $\tilde{T}$ depends on the problem parameter η, the overlap in the method, the mesh parameter h and the lowest frequency along the interface, $k_{\min}$, which in our case would be $k_{\min} = \pi$, since this is the lowest possible mode at the interfaces fixed at $y = 0$ and $y = 1$ by a Dirichlet condition. In [9], the hierarchy of choices in Table 4.1 was derived for h small for the PDE (4.1). Figure 4.2 displays the effect of replacing the classical subdomain matrices A_j by the optimized subdomain matrices $\tilde{A}_j$, $j = 1,2$, on the convergence of RAS for the model problem (4.1) on the unit square with $\eta = 1$ and $h = 1/30$. We applied the asymptotic formulas from Table 4.1 for the various choices of the parameters p and q in the new interface blocks $\tilde{T}$ (4.2) of the optimized subdomain matrices $\tilde{A}_j$. Clearly, the convergence of RAS is greatly enhanced with the new subdomain matrices $\tilde{A}_j$, and exchanging the interface blocks T_η by $\tilde{T}$ does not change the number of operations per iteration in any way.

There is an interesting observation concerning the overlap: in the experiment above, we used an overlap at the matrix level of two blocks in the definition of the restriction operators R_j, $j = 1,2$, which corresponds to the drawing in Figure 4.1 and is the smallest possible satisfying the overlap condition in Theorem 3.4. This corresponds for the classical RAS method to an overlap of $3h$, because the matrices $B_{12} = B_{21} = h^{-2}I$, which pick up the Dirichlet values from the other subdomains in (2.11), are a distance $3h$ apart in physical space, see the decomposition in Figure

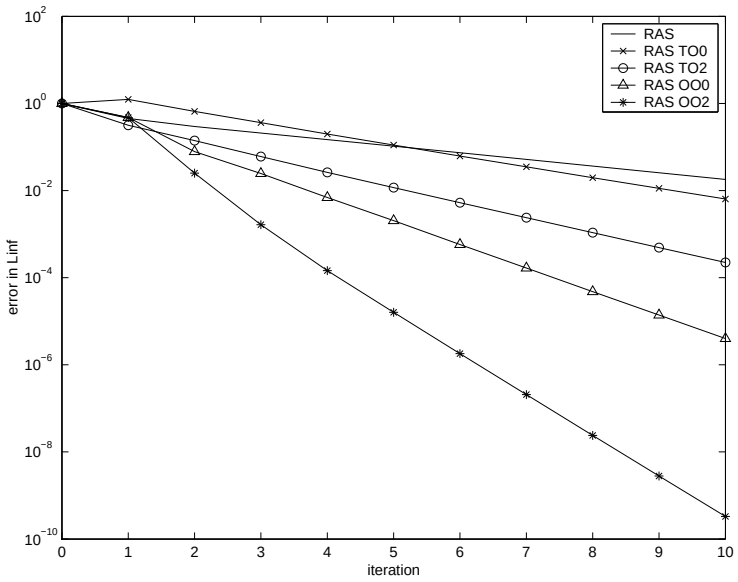

FIG. 4.2. *Convergence curves of classical RAS (top), with overlap $3h$, compared to the hierarchy of optimized RAS methods with overlap h.*

4.1. This distance remains the same in optimized RAS, but the values picked up by the new $\tilde{B}_{12}$ and $\tilde{B}_{21}$ now include in addition to the ones picked up by B_{12} and B_{21} values in the neighboring row corresponding to the changes in $\tilde{A}_j$, and the values from B_{12} and B_{21} are used for the normal derivatives inside the neighboring domain. This implies that the physical interface has shifted by h on each subdomain, and hence the physical overlap is reduced by $2h$, and is thus only of size h for ORAS. In other words, the new physical interface is now on the grid lines denoted by a and b in Figure 4.1. We therefore used $C = 1$ for overlap h in the formulas in Table 4.1 to determine the parameters p and q. This shows that ORAS can not be used without physical overlap, because we chose the smallest overlap according to Theorem 3.4, even though optimized Schwarz methods can be used without overlap.

Another interesting equivalence is now apparent: from formula (4.2), we observe that the new interface blocks $\tilde{T}$ and the classical interface blocks T coincide, if one chooses

$$p = \frac{2 + \eta h^2}{2h}, \quad q = \frac{h}{2}, \tag{4.3}$$

and thus the optimized RAS method with parameters (4.3) and overlap h is identical to the classical RAS method with overlap $3h$. The numerical results in Figure 4.2 demonstrate however that the reduction in overlap is more than compensated for by a good choice of the parameters p and q.

In Figure 4.3, we illustrate the impact of the new subdomain matrices on the convergence of MS. The error is plotted on top for the same configuration as in the previous experiments with RAS. As expected, the convergence is about two times faster then RAS. At the bottom we show the results obtained for OMS with zero overlap, which corresponds in the classical case to an overlap of $2h$. Here, one can see that the Taylor transmission conditions are not effective enough to compensate

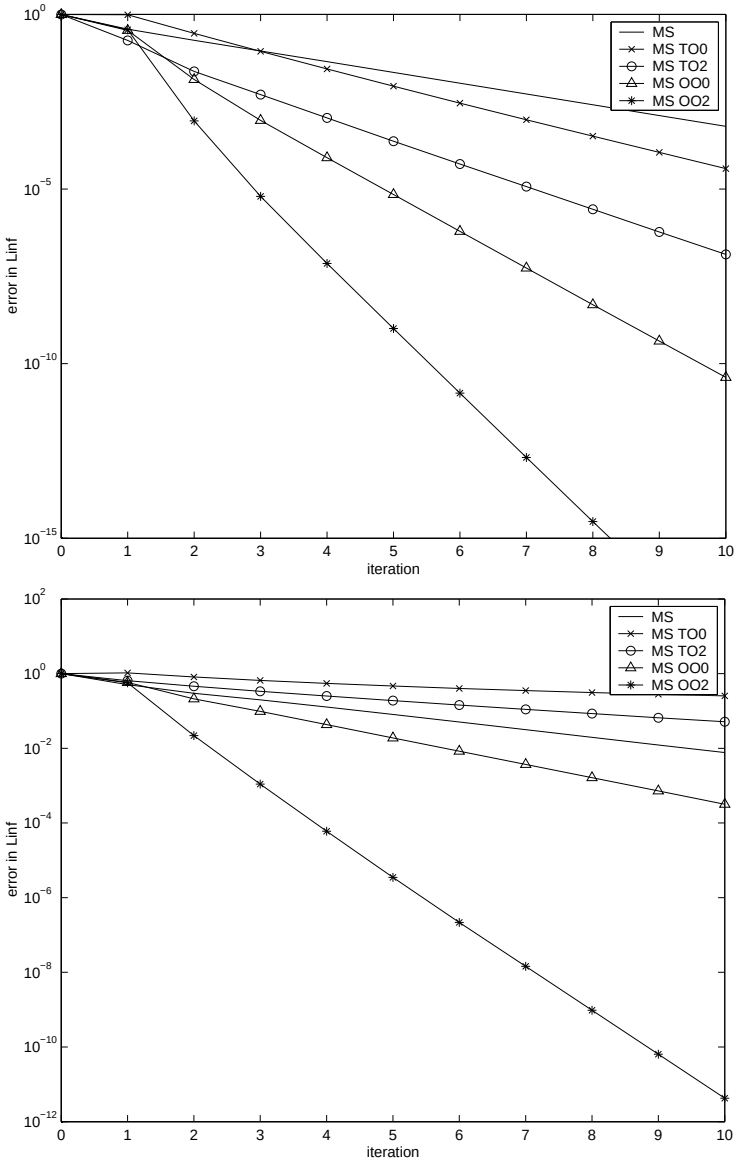

FIG. 4.3. *Convergence curves of classical MS compared to the hierarchy of optimized MS methods, on the top for overlap h ($3h$ for classical MS), and at the bottom for zero overlap ($2h$ for classical MS).*

for the loss of overlap, even though asymptotically they are comparable to classical MS with overlap $2h$, as shown in [9]. The optimized transmission conditions without overlap again improve upon the classical results with overlap by a large margin.

4.2. Spectral Elements. In a nodal spectral element discretization, the computational domain Ω is partitioned into J quadrilateral elements Ω_j in which the dependent and independent variables are approximated by N–th order tensor-product polynomial expansions. A function $u : \mathbb{R}^2 \to \mathbb{R}$ is expanded, on element Ω_j, in terms

of the N–th degree Lagrangian interpolants h_i as defined in [21],

$$u^h(\mathbf{x}(r_1^j, r_2^j))|_{\Omega_j} \equiv u_j(\mathbf{x}(r_1^j, r_2^j)) \equiv \sum_{k=0}^{N}\sum_{l=0}^{N} (\mathbf{u}_j)_{kl}\, h_k(r_1^j(\mathbf{x}))\, h_l(r_2^j(\mathbf{x})), \tag{4.4}$$

where $\mathbf{x} \to (r_1^j(\mathbf{x}), r_2^j(\mathbf{x}))$ is an affine transformation from the quadrilateral element Ω_j, on the original domain, to the reference element $[-1,1]\times[-1,1]$ and $(\mathbf{u}_j)_{kl}$ are the nodal basis coefficients defined at the Gauss-Lobatto Legendre (GLL) quadrature points $\{\xi_i\}_{i=0}^N$. The weak formulation is obtained by integrating the differential equation (4.1) with respect to test functions in $H_0^1(\Omega)$ if Dirichlet conditions are assumed on the physical boundary $\partial\Omega$. By directly evaluating integrals using Gaussian quadrature, the generalized Galerkin problem consists of finding u in $X^N \equiv \mathbb{P}_{N,J}^2 \cap H_0^1(\Omega)$ such that

$$a^h(\phi, u) \equiv \eta(\phi, u)_{GLL} + (\nabla\phi, \nabla u)_{GLL} = (\phi, f)_{GLL} \equiv f^h(\phi) \tag{4.5}$$

for all ϕ in X^N where the polynomial space $\mathbb{P}_{N,J}^2$ of degree N is defined as in [8]. The integrals are obtained as follows:

$$(f,g)_{GLL} \equiv \sum_{j=1}^{J}\sum_{k,l=0}^{N} f(\mathbf{x}^j(\xi_k,\xi_l))|_{\Omega_k} \cdot g(\mathbf{x}^j(\xi_k,\xi_l))|_{\Omega_j}\ |\mathcal{J}^j(\xi_k,\xi_l)|\rho_k\rho_l, \tag{4.6}$$

where $|\mathcal{J}^j(\xi_k,\xi_l)|$ is the Jacobian of the transformation $\mathbf{x}^j(\mathbf{r})$ and $\{\rho_i\}_{i=0}^N$ are the GLL weights associated with the quadrature points $\{\xi_i\}_{i=0}^N$. In our numerical experiments, the Jacobian is simply $\frac{h^2}{4}$ for all quadrilaterals Ω_j.

In order to construct a non-overlapping algorithm, the augmented system must be explicitly derived to find an expression for the matrices $\tilde{B}_{ij}$. This can be accomplished in two different ways. The first approach employs the weak formulation directly on each domain. The second is simply to use the consistency relation in Lemma 3.2 and to construct the matrices $\tilde{B}_{jk}$. The latter can be extracted by specifying the form of the operator $\tilde{A}_j$ on each element. The complete derivation can be found in [26] for general curvilinear domains. Assuming that the spectral elements Ω_j coincide with the subdomains and that a general transmission condition between each element is used,

$$\left[\frac{\partial u_j}{\partial \mathbf{n}} + T(u_j,p,q,\tau)\right]_{\Gamma_{ij}}^{n+1} = \left[\frac{\partial u_i}{\partial \mathbf{n}} + T(u_j,p,q,\tau)\right]_{\Gamma_{ij}}^{n}$$

where $T(u_j,p,q,\tau) \equiv pu_j - q\frac{\partial^2 u_j}{\partial \tau^2}$, we now construct the optimized additive Schwarz algorithm. At the continuous level, the optimized Schwarz algorithm solves the following problem for u_j^{n+1} on each Ω_j

$$\begin{aligned}
\eta u_j^{n+1} - \Delta u_j^{n+1} &= f_j(x,y) && \text{in } \Omega_j,\\
T(u_j^{n+1},p,q,\tau) + \tfrac{\partial u_j^{n+1}}{\partial \mathbf{n}_{jl}} &= T(u_l^n,p,q,\tau) + \tfrac{\partial u_l^n}{\partial \mathbf{n}_{jl}} && \text{on } \Gamma_{jl} \equiv \partial\Omega_j \cap \partial\Omega_l,\\
u_j^{n+1} &= g(x,y) && \text{on } \partial\Omega_j \cap \partial\Omega,
\end{aligned} \tag{4.7}$$

where $l \in \mathcal{N}(\Omega_j)$, which represents the set of integers containing the indices of the elements which are neighbors of Ω_j sharing a complete edge or a vertex, $\mathbf{n}_{jl}$ is a normal

vector pointing from element Ω_j to element Ω_l along the boundary Γ_{jl} and superscript n denotes the iterate of the Schwarz algorithm. After some manipulation, one step of the discrete optimized Schwarz algorithm for the spectral element discretization is to find u_j^{n+1} in $X_j^N \equiv \mathbb{P}_{N,J}^2 \cap H^1(\Omega_j) \cap H_0^1(\Omega)$ such that

$$a_j^h(u_j^{n+1},\phi_j)+\sum_{l\in\mathcal{N}(\Omega_j)} <\phi_j, T(u_j^{n+1},p,q,\tau)>|_{\Gamma_{jl}} = f_j^h(\phi_j)+\sum_{l\in\mathcal{N}(\Omega_j)} f_l^h(\phi_l|_{\Gamma_{jl}}) \\ -\sum_{l\in\mathcal{N}(\Omega_j)} a_l^h(u_l^n,\phi_l|_{\Gamma_{jl}})+\sum_{l\in\mathcal{N}(\Omega_j)} <\phi_l, T(u_l^n,p,q,\tau)>|_{\Gamma_{jl}} \tag{4.8}$$

for all ϕ_j in X_j^N. The bracket $<\cdot,\cdot>|_{\Gamma_{jl}}$ is the discrete one dimensional integral on an edge or vertex Γ_{jl} performed using the GLL quadrature and $a_j^h(\cdot,\cdot)$ is identical to $a^h(\cdot,\cdot)$ with the exception that the sum is taken for element Ω_j only with the same convention for $f_j^h(\cdot)$. The notation $\phi_l|_{\Gamma_{jl}}$ denotes the trace of the test function on the edge Γ_{jl}, including end points, and $\phi_l|_{\Gamma_{jl}}(x) = \phi_j|_{\Gamma_{jl}}(x)$ since, at convergence, the functions must be in $H_0^1(\Omega)$ see [19] for example.

REMARK 4. *The vertex integrals are performed in the same way as their edge or surface counterparts except that the test function is non-zero only at the vertex point and zero at all other collocation points. Using the basis described in [8] such a test function for the vertex situated at* $-(1,1)$*, on the reference element, would be* $h_0(r_1^j)h_0(r_2^j)$. The proposed algorithm (4.8) is a relaxation of the assembly procedure at the heart of any finite element method. The following links to Lemma 3.2 can be established:

$$\underline{\phi}_j^T \tilde{A}_j \hat{R}_j \hat{\mathbf{u}} = a_j^h(\mathbf{u}_j,\underline{\phi}_j)+\sum_{l\in\mathcal{N}(\Omega_j)} <\underline{\phi}_j, T(\mathbf{u}_j,p,q,\tau)>|_{\Gamma_{jl}} \tag{4.9}$$

$$\underline{\phi}_j^T \sum_{l=1}^{J} \tilde{B}_{jl}\hat{R}_l\hat{\mathbf{u}} = -\sum_{l\in\mathcal{N}(\Omega_j)} a_l^h(\mathbf{u}_l,\underline{\phi}_l|_{\Gamma_{jl}})+\sum_{l\in\mathcal{N}(\Omega_j)} <\underline{\phi}_l, T(\mathbf{u}_l,p,q,\tau)>|_{\Gamma_{jl}} \tag{4.10}$$

$$\underline{\phi}_j^T \hat{R}_j A\hat{\mathbf{u}} = a_j^h(\mathbf{u}_j,\underline{\phi}_j)+\sum_{l\in\mathcal{N}(\Omega_j)} a_l^h(\mathbf{u}_l,\underline{\phi}_l|_{\Gamma_{jl}}) \tag{4.11}$$

$$\underline{\phi}_j^T \hat{R}_j \hat{\mathbf{f}} = f_j^h(\underline{\phi}_j)+\sum_{l\in\mathcal{N}(\Omega_j)} f_l^h(\underline{\phi}_l|_{\Gamma_{jl}}) \tag{4.12}$$

for all $1 \le j \le J$ and vector $\underline{\phi}_j$ such that $\mathbf{u}_j = \hat{R}_j\hat{\mathbf{u}}$. Finally, the preconditioned system can be written as

$$(I-\sum_{j=1}^{J}\hat{R}_j^T\tilde{A}_j^{-1}\sum_{l=1}^{J}\tilde{B}_{jl}\hat{R}_l)\hat{\mathbf{u}} = \sum_{j=1}^{J}\hat{R}_j^T\tilde{A}_j^{-1}\hat{R}_j\hat{\mathbf{f}}. \tag{4.13}$$

Notice that no Lagrange multipliers were introduced to find the value of the normal derivative at corners as in [15]. Coerciveness must be ensured for each local problem. The coefficient $p = O(\sqrt{\eta})$, in the case of a zeroth order Taylor approximation can be too small for spectral elements. For a zeroth order optimized p this seems not to be a problem. This was also observed in the case of locally discontinuous Galerkin approximations where good bounds on the penalty coefficient p are available for triangles of degree up to 8 (see [24] for instance).

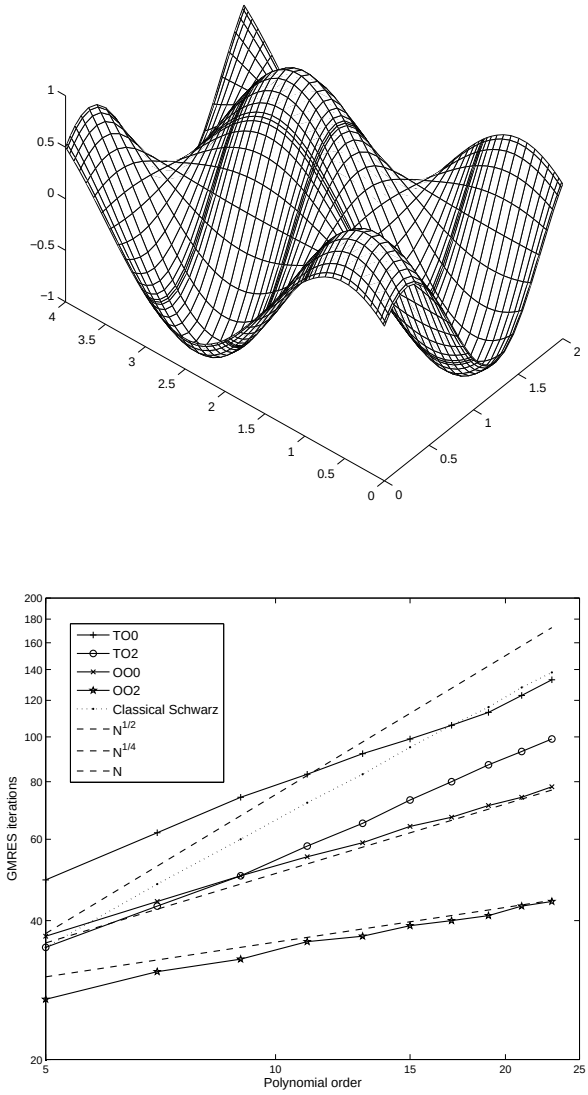

FIG. 4.4. Top: *SEM solution to the positive definite Helmholtz problem on a biperiodic domain for a C^∞ right hand side, and polynomial order* 15 *and* 8 *spectral elements.* Bottom: *Number of GMRES iterations for different choices of preconditioning and polynomial degree for the augmented SEM matrix. The expected asymptotic behavior of each preconditioner is also displayed.*

In order to test the spectral element optimized Schwarz algorithm, the positive definite Helmholtz problem is solved with the C^∞ right hand side

$$f(x,y) = (1 + 5\pi^2/4)\sin(\pi x + \pi/4)\sin(\pi y/2 + \pi/4). \tag{4.14}$$

The domain Ω is the rectangle $[0,2]\times[0,4]$. The solution is depicted in the top panel of Figure 4.4. In the case of GMRES, in the most favorable situation, one should expect

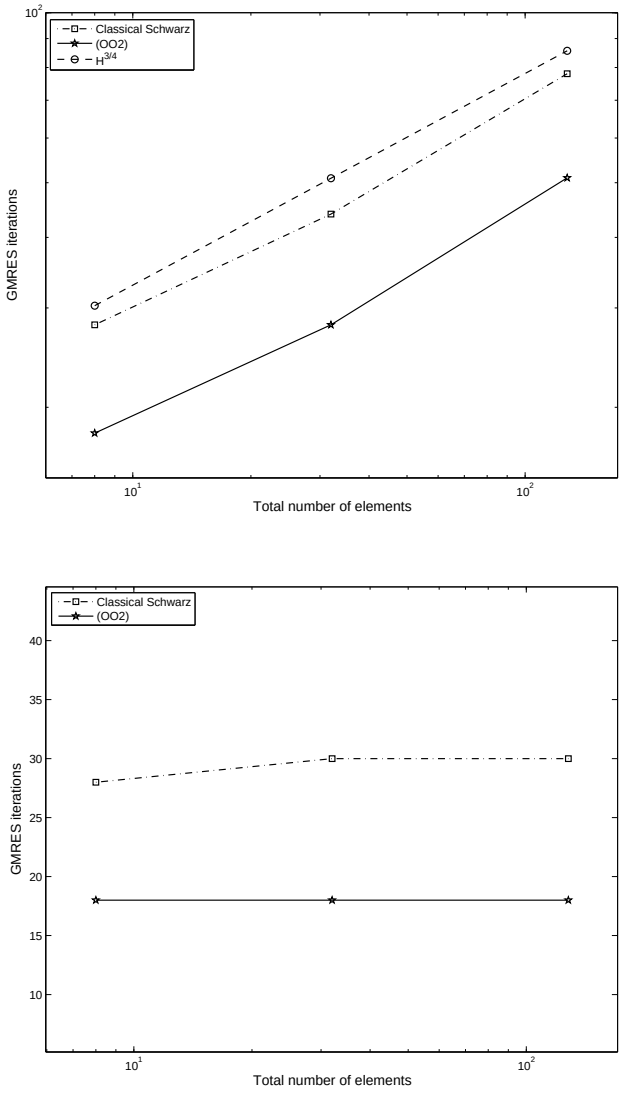

FIG. 4.5. Top and bottom: *number of GMRES iterations for classical Schwarz and optimized Schwarz (OO2) using polynomial degree $N = 5$ and a varying number of elements and no coarse solver.* Bottom only: *the formula used for η is $\frac{J}{4}(\frac{N}{4})^4$ where J is the number of elements and N the polynomial degree.*

the number of iterations to be proportional to the square root of the condition number of the preconditioned spectral element matrix $\kappa(M^{-1}A)$. The bottom panel of Figure 4.4 depicts the number of GMRES iterations with respect to the polynomial degree N. In all tests, a starting vector with random entries between $[0, 1]$ was employed, which guarantees that all frequencies are contained in the error during the iteration and is important when verifying asymptotics, see [9]. For a classical Schwarz preconditioner applied to the augmented system, the asymptotic behavior in the number of iterations reveals the expected growth in the condition number, namely, $\kappa(M_{AS}^{-1}A) = O(N^2)$ see

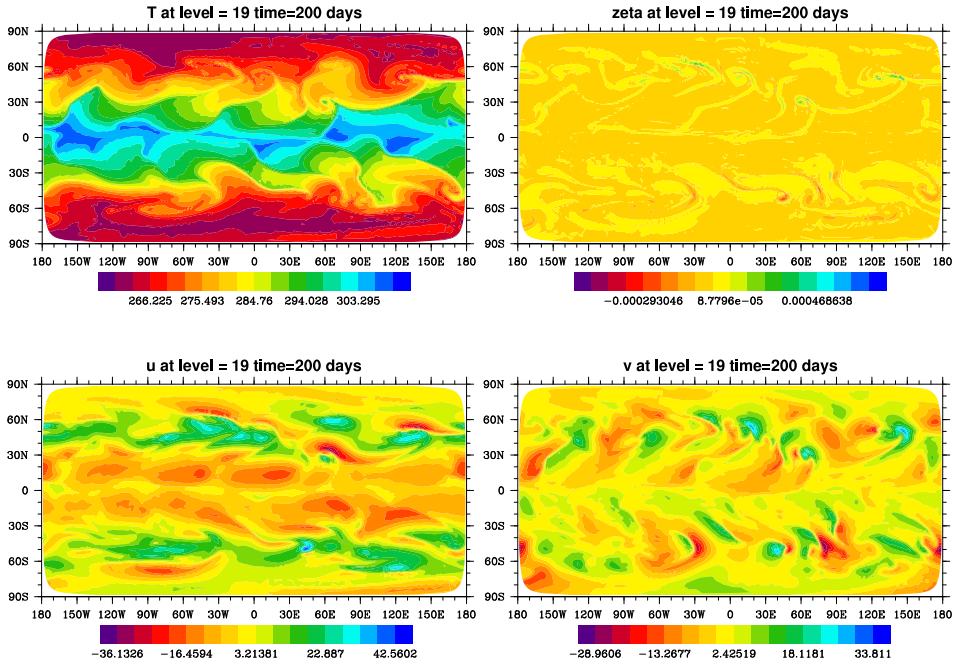

FIG. 4.6. *Held Suarez test, temperature field, vorticity and velocities (latitudinal and longitudinal) at the surface of the planet after 200 days of simulation obtained with the spectral element General Circulation Model (GCM).*

for instance [31]. For the zeroth order optimized Robin transmission condition, the convergence rate is $\kappa(M_{OO0}^{-1}A) = O(N)$ which is an order N better than the classical Schwarz or a sub-structuring method. The most dramatic gains are obtained when the second order tangential derivatives are added to the transmission operator. A very slow growth in the condition number is observed: $\kappa(M_{OO2}^{-1}A) = O(\sqrt{N})$. This result is in agreement with the theory developed in [18]. In addition to the change in the asymptotic behavior, the number of iterations also decreases for a fixed polynomial degree and an increasingly sophisticated transmission operator.

The behavior of the algorithm with respect to the number of spectral elements, which equals the number of subdomains, is considered next. In the top panel of Figure 4.5, if the parameter η is kept fixed, then the number of iterations behaves like $O(H^{3/4})$ which is well within the limits established in [18]. However, if the parameter η is changed following the rule $O(JN^4)$, where J is the number of spectral elements in 2D and N is the polynomial degree, then the number of iterations is independent of both H and N (see bottom panel of Figure 4.5). This was observed by Cai in [2] for the classical Schwarz method, and by Qin and Xu in [18] for optimized Schwarz methods in the general case.

The method was also tested in an atmospheric general circulation model (GCM). At each semi-implicit Eulerian time step, a positive definite Helmholtz problem must be solved (see [20]). The computational domain is the projection of a cube onto the surface of the sphere where the primitive equations are solved in a thin layer above the surface. Vertical acceleration is ignored due to the hydrostatic assumption. Details of the semi-implicit time discretization with spectral elements can be found in Thomas and Loft [30]. The vertical finite difference discretization results in a set of uncou-

pled positive definite Helmholtz problems where the parameter η in (4.1) depends on the vertical structure of the atmosphere. It should be noted that the problem stiffness increases with height above the surface due to the increasing linear gravity wave speeds. Here, the test proposed by Held and Suarez [13] is considered where an analytical solution is not available. In the experimental setup, a diabatic heating is prescribed together with a frictional forcing. This gives rise to climate simulations similar to those obtained with more complex physics, see Figure 4.6. The domain is partitioned into 6144 spectral elements and each one of these elements is considered as a subdomain in the optimized Schwarz algorithm. A fifth order polynomial expansion is employed on each element. Parallel performance results obtained on the IBM Blue Gene machine are presented in Figure 4.7 and are shown to be competitive with the explicit time-stepping approach in terms of scaling. For integration rates of the model for various computer architectures see [4] and [26]. The number of operations, or computational cost, in 2D, to perform a preconditioned matrix vector multiplication behaves asymptotically like $O(JN^3)$ as compared to $O(JN^4)$ when a fast diagonalization method cannot be employed. The speedup of the explicit time stepping was scaled with respect to the semi-implicit. For an overview of the machine, its two modes (coprocessor and virtual node) and techniques for optimizing the communication patterns, consult [1]. Note that the augmented system formulation enables one to store only $O(N^3)$ matrix entries per spectral element for application of the inverse instead of the $O(N^4)$ entries required in the case of an LU factorization. Since the L2 cache available on the Blue Gene machine is rather small (2KB), the savings are advantageous. No coarse solver is needed in the GCM. This is a consequence of the semi-implicit time discretization. The model time-step is restricted by the advective Courant-Friedrich-Levy condition which scales the parameter $\eta = \eta(\Delta t)$ as $O(JN^4)$. On massively parallel computers such as the Blue Gene machine, avoiding the coarse solve is of uttermost importance. A quantification of how a coarse solver affects parallel performance on such machines can be found in [32].

5. Conclusion. Our presentation showed how the one-level restricted additive Schwarz and multiplicative Schwarz algorithms can be modified to increase their respective convergence rates in the context of multiple domains. For the optimized restricted additive Schwarz algorithm, a condition on the overlap is required to produce optimized iterates. It was also shown how an augmented system can be constructed to generate optimized iterates for domains with non-overlapping regions. Theoretical results were obtained at the algebraic level and are independent of the underlying spatial discretization. Finite difference and high-order spectral element examples document the simplicity and significant convergence acceleration. The augmented system is appropriate for high-order methods, where the construction of an overlapping grid is cumbersome and technically challenging. For zeroth order optimized transmission conditions, the condition number of the preconditioned spectral element matrix is asymptotically N times better than the condition number resulting from a classical Schwarz method or a sub-structuring method with similar computational cost. For a second order optimized transmission operator, the behavior with respect to the polynomial order confirms the asymptotic results found in [9, 18]. When the stiffness induced by η in the model equation is modified following the Eulerian semi-implicit GCM advective time step restriction, then all block preconditioners are optimal with respect to H refinement: alleviating the use of a coarse solver. Regardless, the second order optimized Schwarz approach yields the smallest number of iterations. Application of the method to a spectral element climate model results in a significant

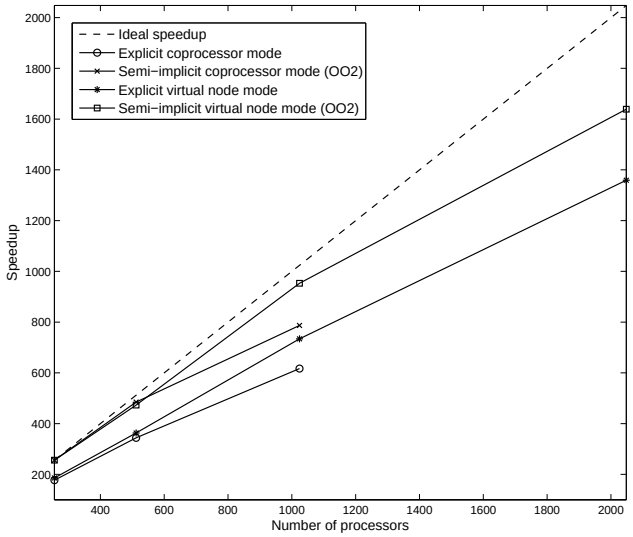

FIG. 4.7. *Speedup for the general circulation model (GCM) on a single rack of the IBM Blue Gene machine for* 6144 *spectral elements, 20 vertical levels and polynomial order* 5.

reduction of the computing time, demonstrating the practicality of the theoretical results. It is conjectured that more realistic sub-grid scale physical forcing will result in a much broader range of unresolved frequencies, in which case the optimized algorithm will be the method of choice.

Acknowledgments. This work was partially supported by NSF CMG[1] grant 0222282 and the DOE[2] CCPP[3]. Traveling funds were made available by the ECSA[4], the Scientific Computing Division, both at NCAR[5], and Geneva University for the first two authors. Computer time was provided by NSF MRI Grant CNS-0421498, NSF MRI Grant CNS-0420873, NSF MRI Grant CNS-0420985, NSF sponsorship of NCAR, the University of Colorado, and a grant from the IBM Shared University Research (SUR) program.

REFERENCES

[1] BHANOT, G., GARA, A., HEILDELBERGER, P., LAWLESS, E., SEXTON, J. C., AND WALKUP, R. Optimizing task layout on the Blue Gene/L supercomputer. *IBM J. Res. & Dev. 49*, 2/3 (2005), 489–500.

[2] CAI, X.-C. Additive Schwarz algorithms for parabolic convection-diffusion equations. *Numer. Math. 60*, 1 (1991), 41–61.

[3] CAI, X.-C., AND SARKIS, M. A restricted additive Schwarz preconditioner for general sparse linear systems. *SIAM Journal on Scientific Computing 21* (1999), 792–797.

[1] National Science Foundation Collaborations in Mathematics and Geosciences
[2] Department of Energy
[3] Climate Change Prediction Program
[4] Early Career Scientist Association
[5] National Center for Atmospheric Research

[4] Dennis, J., Fournier, A., Spotz, W. F., St-Cyr, A., Taylor, M. A., Thomas, S. J., and Tufo, H. High-resolution mesh convergence properties and parallel efficiency of a spectral element atmospheric dynamical core. *Int. J. High Perform. Comput. Appl. 19*, 3 (2005), 225–235.

[5] Dryja, M., and Widlund, O. B. An additive variant of the Schwarz alternating method for the case of many subregions. Tech. Rep. 339, Department of Computer Science, Courant Institute, 1987.

[6] Dubois, O. Optimized Schwarz methods with Robin conditions for the advection-diffusion equation. In *Domain Decomposition Methods in Science and Engineering XVI* (2007), D. E. Keyes and O. B. Widlund, Eds., vol. 55 of *Lecture Notes in Computational Science and Engineering*, Springer-Verlag. Berlin-Heidelberg, pp. 181–188.

[7] Efstathiou, E., and Gander, M. J. Why restricted additive Schwarz converges faster than additive Schwarz. *BIT Numer. math. 43*, 3 (2003), 945–959.

[8] Fischer, P. F. An overlapping Schwarz method for spectral element solution of the incompressible Navier-Stokes equations. *J. Comput. Phys. 133*, 3 (1997), 84–101.

[9] Gander, M. J. Optimized Schwarz methods. *SIAM J. Numer. Anal. 44*, 2 (2006), 699–731.

[10] Gander, M. J., Halpern, L., and Magoulès, F. An optimized Schwarz method with two-sided Robin transmission conditions for the Helmholtz equation. *Int. J. for Num. Meth. in Fluids* (2006). to appear.

[11] Gander, M. J., Halpern, L., Magoulès, F., and Roux, F.-X. Patch substructuring methods. *Comptes Rendus de l'Academie des Sciences* (2007). submitted.

[12] Gander, M. J., Magoulès, F., and Nataf, F. Optimized Schwarz methods without overlap for the Helmholtz equation. *SIAM J. Sci. Comput. 24*, 1 (2002), 38–60.

[13] Held, I. H., and Suarez, M. J. A proposal for the intercomparison of the dynamical cores of atmospheric general circulation models. *Bull. Amer. Met. Soc. 75* (1994), 1825–1830.

[14] Japhet, C., Nataf, F., and Rogier, F. The optimized order 2 method. application to convection-diffusion problems. *Future Generation Computer Systems FUTURE 18* (2001).

[15] Kimn, J.-H. A convergence theory for an overlapping Schwarz algorithm using discontinuous iterates. *Numerische Mathematik 100*, 1 (2005), 117–139.

[16] Lions, P.-L. On the Schwarz alternating method. I. In *First International Symposium on Domain Decomposition Methods for Partial Differential Equations* (Philadelphia, PA, 1988), R. Glowinski, G. H. Golub, G. A. Meurant, and J. Périaux, Eds., SIAM, pp. 1–42.

[17] Magoulès, F., Roux, F.-X., and Salmon, S. Optimal discrete transmission conditions for a non-overlapping domain decomposition method for the Helmholtz equation. *SIAM Journal on Scientific Computing 25*, 5 (2004), 1497–1515.

[18] Qin, L., and Zhang, X. On a parallel Robin-type nonoverlapping domain decomposition method. *SIAM J. Numer. Anal. 44*, 6 (2006), 2539–2558.

[19] Quarteroni, A., and Valli, A. *Numerical Approximations of Partial Differential Equations*, 2 ed., vol. 23 of *Springer series in Computational Mathematics*. Springer-Verlag, 1997.

[20] Robert, A. J. A semi-Lagrangian and semi-implicit numerical integration scheme for the primitive meteorological equations. *J. Met. Soc. Jpn. 60* (1982), 319–325.

[21] Ronquist, E. *Optimal Spectral Element Methods for the Unsteady Three-Dimensional Incompressible Navier-Stokes Equations*. PhD thesis, M.I.T., Cambridge, MA, 1988.

[22] Roux, F.-X., Magoules, F., Salmon, S., and Series, L. Optimization of interface operator based on algebraic approach. In *14th International Conference on Domain Decomposition Methods, Cocoyoc, Mexico* (2002), I. Herrera, D. E. Keyes, O. B. Widlund, and R. Yates, Eds.

[23] Schwarz, H. A. Über einen Grenzübergang durch alternierendes Verfahren. *Vierteljahrsschrift der Naturforschenden Gesellschaft in Zürich 15* (May 1870), 272–286.

[24] Shahbazi, K. Short note: An explicit expression for the penalty parameter of the interior penalty method. *Journal of Computational Physics 205* (2005), 401–407.

[25] Smith, B. F., Bjørstad, P. E., and Gropp, W. *Domain Decomposition: Parallel Multilevel Methods for Elliptic Partial Differential Equations*. Cambridge University Press, 1996.

[26] St-Cyr, A. Optimized Schwarz preconditionning for a semi-implicit spectral elements GCM. In preparation, 2007.

[27] St-Cyr, A., Dennis, J. M., Loft, R., Thomas, S., Tufo, H., and Voran, T. Early experiences with the 360TF IBM BlueGene/L platform. *International Journal of Computational Methods* (2007). Accepted for publication.

[28] St-Cyr, A., Gander, M. J., and Thomas, S. J. Optimized restricted additive Schwarz methods. In *Domain Decomposition Methods in Science and Engineering XVI* (NewYork, NY, 2007), O. B. Widlund and D. E. Keyes, Eds., vol. 55 of *Lecture Notes in Computational Science and Engineering*, Springer-Verlag. Berlin-Heidelberg, pp. 213–220.

[29] TANG, W. P. Generalized Schwarz splittings. *SIAM J. Sci. Stat. Comput. 13* (1992), 573–595.
[30] THOMAS, S. J., AND LOFT, R. D. Semi-implicit spectral element atmospheric model. *J. Sci. Comput. 17* (2002), 339–350.
[31] TOSELLI, A., AND WIDLUND, O. *Domain Decomposition Methods-Algorithms and Theory.* Springer series in Computational Mathematics. Springer-Verlag, 2005.
[32] TUFO, H. M., AND FISCHER, P. F. Fast parallel direct solvers for coarse grid problems. *J. Parallel Distrib. Comput. 61* (2001), 151–177.
[33] WILDERS, P., AND BRAKKEE, E. Schwarz and Schur: an algebraical note on equivalence properties. *SIAM J. Sci. Comp. 20*, 6 (1999), 2297–2303.